Nigerian Journal of Physics (NJP)
ISSN online: 3027-0936
ISSN print: 1595-0611
DOI: https://doi.org/10.62292/njp.v35i2.2026.589
Volume 35(2), June 2026

Hydrogeophysical Assessment of Subsurface Controls on Gully Erosion Using Electrical Resistivity Methods in Orlu, Southeastern Nigeria

[1]Obinna C. Dinneya, *[1]Chukwuebuka N. Onwubuariri, [1]Esomchi U. Nwokoma, [2]Stephen O. Akidi and [1]Joshua U. Ugwu

[1]Department of Physics, Michael Okpara University of Agriculture, Umudike, Abia State, Nigeria.
[2]Department of Geology, Michael Okpara University of Agriculture, Umudike, Abia State, Nigeria.

*Corresponding Author's Email: Onwubuariri.chukwuebuka@mouau.edu.ng
ORCID: https://orcid.org/0000-0003-3689-9065

ABSTRACT

Gully erosion constitutes a critical environmental threat in Orlu, southeastern Nigeria, yet the subsurface controls governing this process remain poorly understood. This study employs a quantitative hydrogeophysical approach to elucidate the mechanisms underlying the region's vulnerability to gully erosion. Twelve Vertical Electrical Sounding (VES) stations were deployed using the Schlumberger array to map subsurface resistivity distribution and lithological characteristics. The acquired data revealed significant geological heterogeneity, with resistivity values ranging from 65 to 44,800 Ωm. With increasing depth, resistivity exhibited a consistent upward trend, commencing at 450 Ωm in the moist topsoil and rising sharply to 18,500 Ωm beyond 50 metres. This vertical transition demarcates a shift from stable surface soils to thick, dry, and unconsolidated sandy formations. The results indicate that approximately 68% of the study area falls within a high-risk zone (resistivity exceeding 5,000 Ωm), which correlates precisely with actively forming gully sites. These high-resistivity sandy layers are highly permeable yet lack cohesive strength, functioning as preferential conduits for subsurface flow and internal piping that progressively destabilises the ground from within. By statistically linking resistivity data to erosion behaviour, this research establishes a predictive framework for identifying erosion-prone sites. The findings demonstrate that effective land management and erosion risk assessment in sedimentary regions cannot be accomplished without integrating hydrogeophysical subsurface data.

Keywords:
Electrical resistivity,
Gully erosion,
Hydrogeophysics,
Subsurface characterization,
Southeastern Nigeria.

INTRODUCTION

Gully erosion stands out as one of the most destructive forms of land degradation across the tropics, and in southeastern Nigeria, it has evolved into a full-scale environmental and economic crisis. This process involves the aggressive washing away of soil along drainage paths, creating massive chasms that tear apart the surface, ruin infrastructure, and strip away fertile farmland. In areas like Orlu, the damage is visible everywhere—roads are cut off, homes are lost, and public utilities are swallowed up, creating a massive hurdle for the region's long-term development (Onwubuariri et al., 2018a; Onwubuariri & Mgbeojedo, 2018).

The formation and growth of gullies are driven by a combination of weather, geology, and human activity. Heavy tropical rainfall, steep slopes, and poor farming practices have long been recognised as contributing factors. More recent work, however, has shifted attention toward subsurface conditions. Subsurface factors – such as the lithological composition and the arrangement of different strata – are now understood to be primary controls on site stability (Revil et al., 2021; Servos & Power, 2024). These hidden characteristics govern water movement through the ground and the cohesion between soil particles.

To investigate the subsurface without excavation, electrical resistivity testing has become a standard tool. The method is effective because it responds to changes in soil type, moisture content, and pore-fluid flow. It allows structural weaknesses that are not visible from the surface to be mapped. In hydrogeophysics, resistivity readings serve as a reliable proxy for grain size and clay content,

which in turn indicate how stable or unstable the ground is (Ekanem et al., 2025).

Recent studies using techniques such as electrical resistivity tomography (ERT) and vertical electrical sounding (VES) consistently point to a common pattern: zones with high resistivity are usually dominated by loose, sandy materials, and these are the areas' most vulnerable to erosion. Such sands tend to have very little cohesion, so water moves through them easily, encouraging internal erosion or "piping", where soil is gradually washed away from within (Nwozor et al., 2025; Revil et al., 2020). By contrast, layers that contain more clay behave quite differently—they tend to hold together better, slow down water movement, and help stabilise the ground and reduce erosion.

Furthermore, studies conducted in similar terrains demonstrate a direct correlation between these resistivity variations and the movement of groundwater, as well as the location of aquifers. When you have highly permeable zones that offer little protection, water soaks in fast, building up pressure that weakens the soil's "grip" and leads to sudden slope failures (Onwubuariri et al., 2018b; Thomas et al., 2023). This really highlights why we can't just look at the surface; we have to combine geophysical data with traditional landscape analysis to obtain the full picture of why the ground is failing.

A key gap in understanding erosion around Orlu through a detailed, quantitative hydrogeophysical lens was addressed. The approach centers on vertical electrical soundings (VES) to map out the subsurface layers and get a clear picture of the hydrogeological setup beneath them. Specifically, how resistivity ties into erosion risk was examined, and the area was divided into meaningful zones of vulnerability. By blending these geophysical insights with direct field observations, the study lays out a solid way to spot trouble spots early, before serious damage sets in, ultimately supporting better planning and land use decisions.

The findings highlight zones with very high resistivity (over 5,000 Ωm) as prime hotspots for concern (Nwozor et al., 2025).These often stem from coarse, porous materials that let water drain quickly while offering little resistance to breakdown, priming the ground for gully development. In investigating these issues, we aim to pin down and measure exactly how subsurface traits drive erosion processes.

Despite growing interest in hydrogeophysical approaches, there remains limited quantitative linkage between subsurface resistivity characteristics and gully erosion mechanisms in southeastern Nigeria. Most existing studies rely heavily on surface observations, with little emphasis on how subsurface properties influence erosion dynamics.

Unlike many earlier studies, which relied largely on qualitative interpretation, this work adopts a semiquantitative approach to analysing resistivity data. In practical terms, this involves defining specific resistivity ranges that correspond to different levels of erosion risk. When these ranges are considered alongside the statistical behaviour of the data and field observations, they provide a more transparent way of understanding how and why erosion develops in the area. Ultimately, this approach pushes the field of hydrogeophysics forward. It moves us away from just describing the problem and toward a consistent, scalable way of measuring and predicting where the next gully might strike.

Geology of the Study Area

The study area sits on the eastern edge of the Niger Delta Basin; a massive sedimentary stretch built from thick layers of Tertiary rock left behind as the ancient coastline pulled back and the delta pushed forward. Essentially, the geology here is a stack of three main layers, the Akata, Agbada, and Benin formations, where the ground becomes increasingly sandy as you move closer to the surface (Onwubuariri et al., 2024; Doust & Omatsola, 1990).

The Benin Formation, commonly known as the Coastal Plain Sands, predominates the subsurface geology in the vicinity of Orlu. This layer mostly consists of a blend of loose, medium-to-coarse sands, intermittently interspersed with thin layers of clay and shale (Onwubuariri et al., 2023; Nwozor et al., 2025). These materials are typically friable and characterised by numerous minute voids (porous), as they have not been compacted into solid rocks, indicative of their origin as deposits from ancient rivers and shallow shorelines (Onwubuariri et al., 2023; Nwozor et al., 2025).

In some spots, the Benin formation rests on the Ogwashi–Asaba Formation, a mix of alternating sands, clays, and bits of lignite coal that show just how much the delta environment shifted over time (Onwubuariri et al., 2023). Taken together, the geological history of this region is a long record of rivers, deltas, and shallow seas doing their work from millions of years ago right up to the present day (Obaje, 2009; Nwajide, 2013).

Those sandy layers in the Benin Formation make for top-notch aquifers, thanks to their high porosity and permeability that speed up water infiltration and groundwater movement (Onwubuariri et al., 2023). The abundance of unconsolidated sand and the scarcity of clay significantly reduce soil cohesion and stability, making the terrain highly susceptible to gully erosion during intense rains and runoff.

The study area is situated within the Benin Formation of the Niger Delta Basin, primarily composed of unconsolidated coastal plain sands with modest clay intercalations. The geological framework illustrated in the regional geological map (Figure 1) underpins comprehension of the elevated resistivity values and erosion vulnerability present in the region.

The prevalence of unconsolidated sandy strata in the Benin Formation is anticipated to yield elevated resistivity values owing to less clay content and diminished ionic conduction. This geological context offers a theoretical framework for understanding resistivity anomalies identified in the research area as indicative of erosion-susceptible zones.

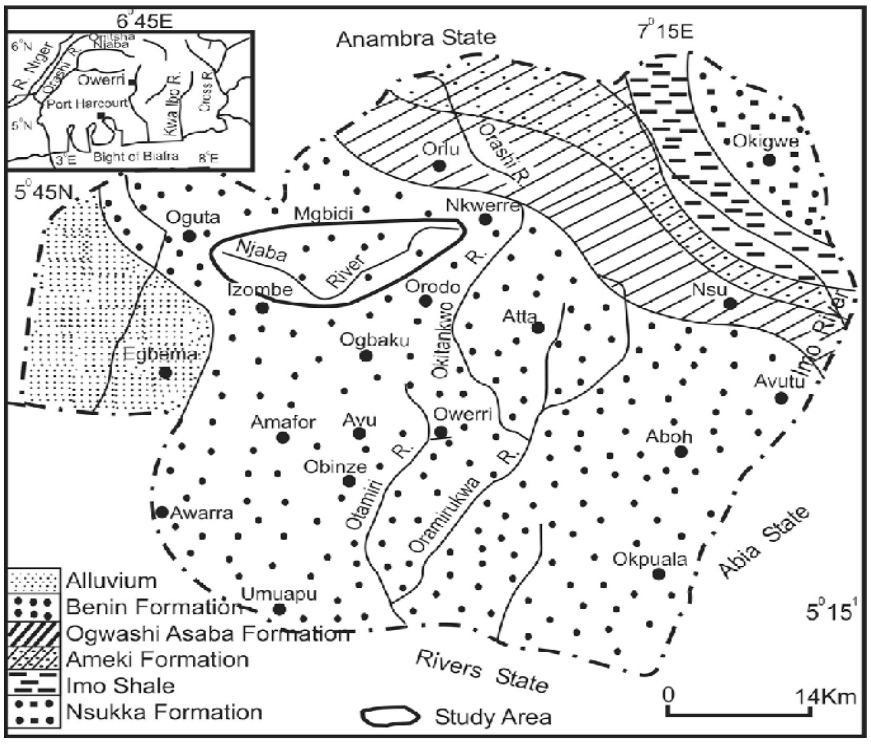

Figure 1: The geology map of the study area

MATERIALS AND METHODS

Field Data Acquisition

Twelve (12) vertical electrical sounding (VES) stations were set up across the study area, using the Schlumberger electrode array. The plan for where to place these stations was driven by practical reality: areas that were accessible were the focus, the local terrain, and, most importantly, how close they were to active gullies. To ensure visibility of the depth of the sites into the earth, the Terrameter SAS series resistivity meter was used, pushing the half-current electrode spacing (AB/2) out to 400 metres.

In this Schlumberger setup, the centre point was fixed, and the current electrodes (A and B) were moved outward in even steps. The potential electrodes (M and N) near the centre were fixed, only adjusting them when the signal started to fade. This specific approach is a favourite in hydrogeophysical work because it's excellent at picking up the different layers beneath the surface (Omeiza et al., 202).

At every site, current electrodes were pumped into the ground through electrodes A and B and measured the resulting voltage drop at M and N. By steadily increasing the distance between the electrodes, we were able to probe deeper and deeper into the subsurface.

To make sure the locations of each VES station were correct, a handheld GPS device was used to record the geographic coordinates. We used the IPI2Win software, which is often used to figure out what resistivity means, to process and invert the data.

Theoretical Basis

The apparent resistivity (ρ_a) of the subsurface was computed using the standard expression in equation 1(Onwubuariri, et al., 2024):

$$\rho_a = K\frac{\Delta V}{I} \quad (1)$$

where:

i. ρ_a = apparent resistivity (Ωm)
ii. ΔV = measured potential difference (V)
iii. I = injected current (A)
iv. K = geometric factor (m)

For the Schlumberger array, the geometric factor is defined as seen in equation 2 (Onwubuariri, et al., 2024):

$$K = \frac{\pi(AB)^2}{4MN} \quad (2)$$

where AB is the current electrode spacing and MN is the potential electrode spacing.

This formulation assumes a horizontally stratified subsurface and is based on Ohm's law, which governs current flow through geological media. Variations in

apparent resistivity reflect contrasts in lithology, porosity, and fluid content (Ibrahim et al., 2025).

Data Processing and Interpretation

The field data were first examined to remove false readings arising from poor electrode contact or noise. The processed apparent resistivity values were then plotted against electrode spacing on a log–log scale to generate sounding curves.

Interpretation was carried out using iterative curve matching and inversion techniques. Initial layer parameters were estimated through manual curve matching, after which computer-assisted inversion was applied to obtain refined models of true resistivity and layer thickness. The inversion process minimises the difference between observed and calculated apparent resistivity values, typically expressed as the root mean square (RMS) error.

Model reliability was maintained by accepting inversion results exclusively when RMS error values remained within acceptable thresholds (generally, 5%), in alignment with established protocols in resistivity interpretation (Ndam et al., 2023). We used lithological information from nearby boreholes, when it was available, to improve our interpretation and make things less confusing. Resistivity data alone may not clearly show what is going on below the surface.

To enhance model reliability, uncertainty analysis was integrated into the inversion process. Numerous inversion iterations were conducted for each VES dataset to evaluate parameter stability, retaining only consistently convergent solutions. Resistivity and thickness variations in layers were observed across iterations to confirm the reliability of the interpreted models. This method reduces the uncertainty associated with resistivity interpretation and enhances confidence in the inferred subsurface structure.

Resistivity-Based Classification of Subsurface Materials

To facilitate interpretation in relation to erosion processes, resistivity values were grouped into hydrogeophysical classes based on established thresholds.

Table 1: Resistivity Classification and Erosion Implication

Resistivity Range (Ωm)	Inferred Lithology	Hydrogeological Property	Erosion Susceptibility
< 500	Clay/saturated materials	Low permeability	Low
500 – 5000	Sandy clay/weathered layer	Moderate permeability	Moderate
> 5000	Dry sand/unconsolidated sediments	High permeability	High

This classification is consistent with the known relationship between resistivity and hydraulic properties, where higher resistivity values typically indicate dry, coarse-grained materials with high infiltration capacity, while lower values are associated with clay-rich or water-saturated formations (Omeiza et al., 2023).

To ensure the robustness of this classification, the defined resistivity thresholds were cross-checked against the statistical distribution of the dataset obtained in this study. The selected ranges correspond closely with the observed quartile distribution of resistivity values, thereby providing empirical support for the classification scheme. This data-driven validation enhances the reliability of the interpretation and ensures consistency between theoretical expectations and field observations.

The classification thresholds were further validated using the statistical distribution of resistivity values obtained in this study, ensuring consistency between empirical data and literature-based ranges.

Integration with Geomorphological Observations

Field observations of gully morphology – including depth, width, and lateral extent – were recorded alongside the geophysical measurements. These observations were then used to establish spatial correspondence between resistivity patterns and active erosion zones. The geophysical and geomorphological data were integrated to improve the reliability of the interpretation and to allow a more robust linkage between subsurface properties and erosion dynamics.

RESULTS AND DISCUSSION

General Resistivity Characteristics of the Study Area

The processed VES data show a wide range of resistivity values across the study area, which shows that the subsurface is very heterogeneous. The values range from 65 Ωm to 44,800 Ωm, which shows that the lithology, moisture content, and degree of consolidation are completely unique.

Statistical measures were obtained from the interpreted resistivity dataset to quantify this variability.

Table 2: Statistical Summary of Resistivity Distribution

Parameter	Value (Ωm)
Minimum	65
Maximum	44,800
Mean	8,920
Median	6,350
Standard Deviation	9,870
Coefficient of Variation (%)	110.6

The large standard deviation (9,870 ohm-m) compared to the mean shows that the data is spread out, which suggests that there are multiple lithological regimes. This range of conditions is very important for studying erosion because different conditions below the ground often cause preferred flow paths and localised instability.

The high coefficient of variation (110.6%) indicates that the subsurface is heterogeneous, consisting of multiple materials with contrasting physical properties layered together. Such variability is typical of sandy sedimentary landscapes, where sorting and deposition processes produce a wide spread in grain size and pore structure. From a geomorphological perspective, this diversity often causes uneven water movement through the soil, creating preferential pathways that can initiate and accelerate erosion.

Depth-Dependent Resistivity Variation

A closer look at how resistivity changes with depth provides further insight into subsurface conditions.

Table 3: Depth–Resistivity Relationship

Depth Range (m)	Average Resistivity (Ωm)
0 – 5	450
5 – 20	2,800
20 – 50	9,600
> 50	18,500

The data consistently indicate that resistivity increases with depth. The resistivity of surface-adjacent layers (0–5 m) is relatively low. This is due to their higher water content and susceptibility to weathering. As depth increases, resistivity rises significantly, indicating that the materials are becoming drier and coarser.

The iso-resistivity contour maps (Figures 2 - 4) distinctly illustrate this trend, exhibiting reduced resistivity values in the shallow strata relative to the deeper strata. These images illustrate the lateral variations in resistivity patterns at various depths. They provide an indication of the location of the data in Table 3. The implication is evident: deeper strata function as highly permeable zones, facilitating the movement of water beneath the surface, potentially compromising the stability of the overlying materials.

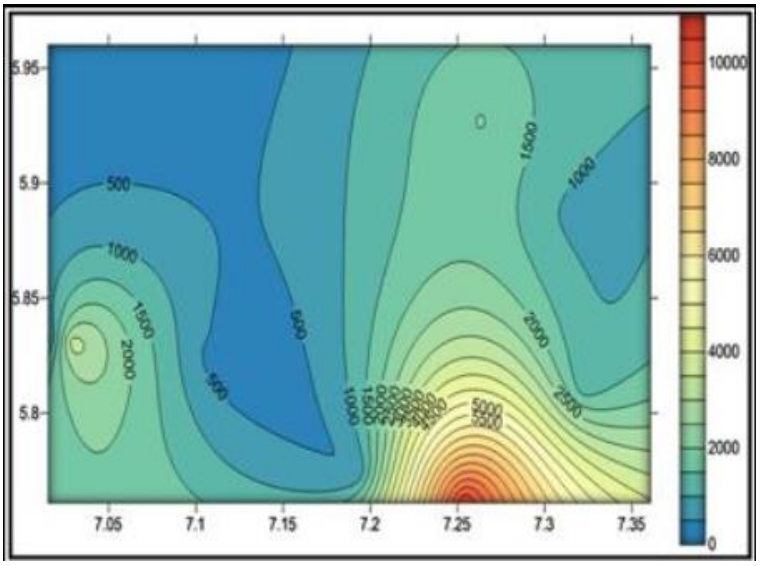

Figure 2: Iso-resistivity contour at the value AB/2 = 5

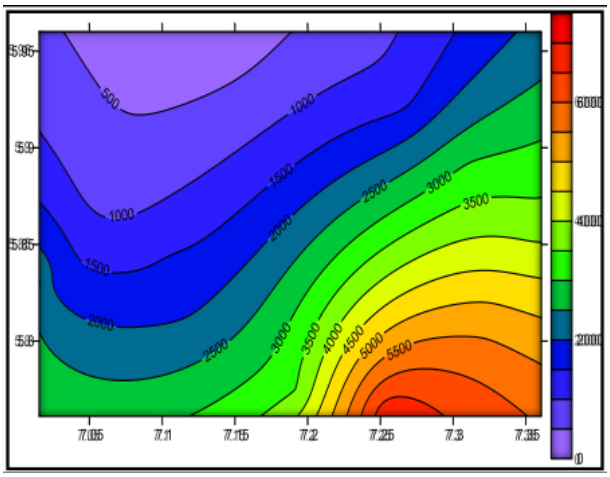

Figure 3: Iso-resistivity contour at the value AB/2 = 125

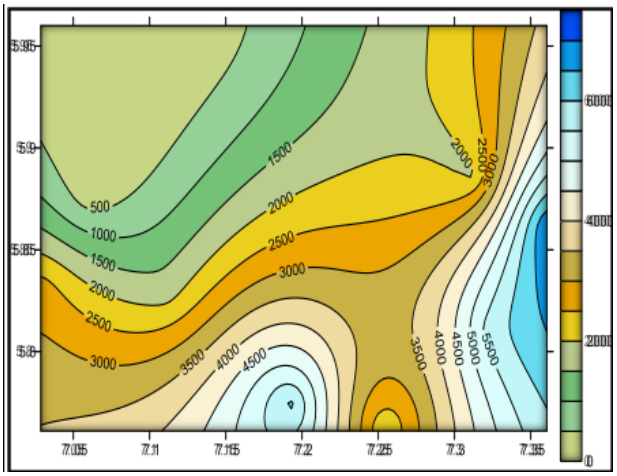

Figure 4: Iso-resistivity contour at the value AB/2 = 250

Geoelectric Layering and Lithological Interpretation

The inversion of VES data reveals a multi-layered subsurface structure, typically consisting of four to six distinct layers.

Table 4: Generalized Geoelectric Layer Parameters

Layer	Resistivity Range (Ωm)	Thickness Range (m)	Interpreted Lithology
1	65 – 800	0.9 – 2.5	Lateritic topsoil
2	800 – 5,000	2.5 – 10	Sandy clay / weathered layer
3	5,000 – 20,000	10 – 45	Medium to coarse sand
4	20,000 – 44,800	45 – 177	Dry, unconsolidated sand

These layered characteristics are visually represented in the layer resistivity contour maps (Figures 5 – 10). Each of these figures corresponds to a specific geoelectric layer and shows how resistivity varies spatially across the study area.

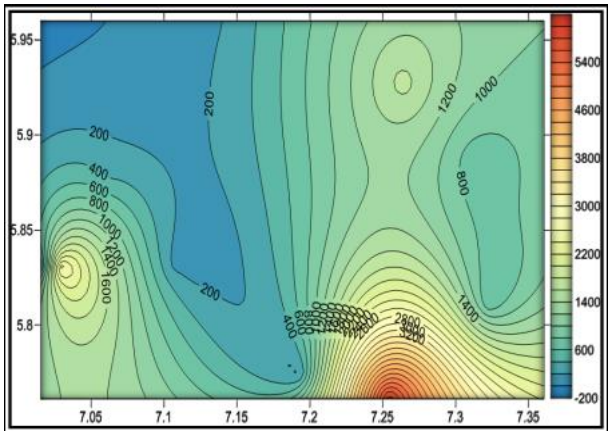

Figure 5: The resistivity contour of the entire 1st layers

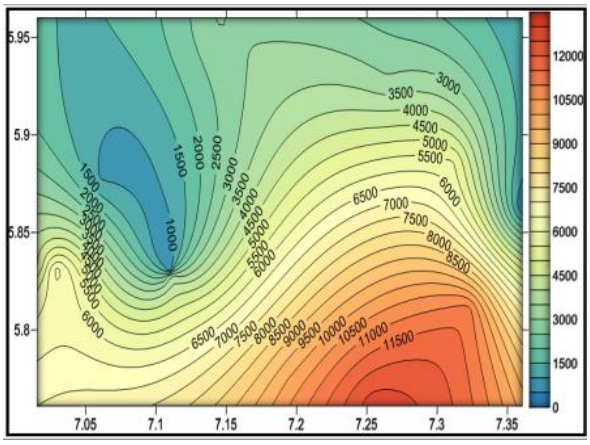

Figure 6: The resistivity contour of the entire 2nd layers

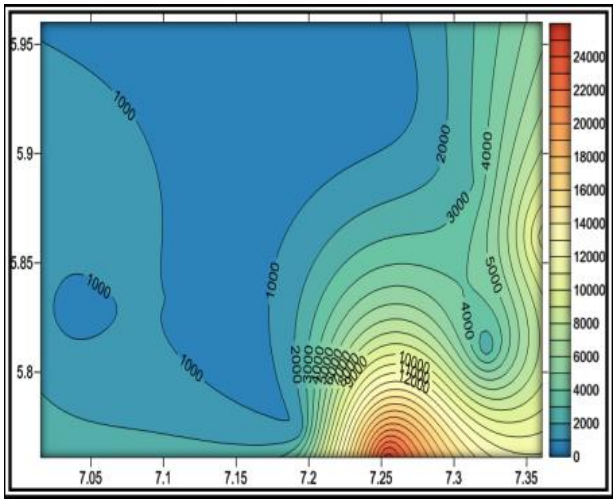

Figure 7: The resistivity contour of the entire 3rd layers

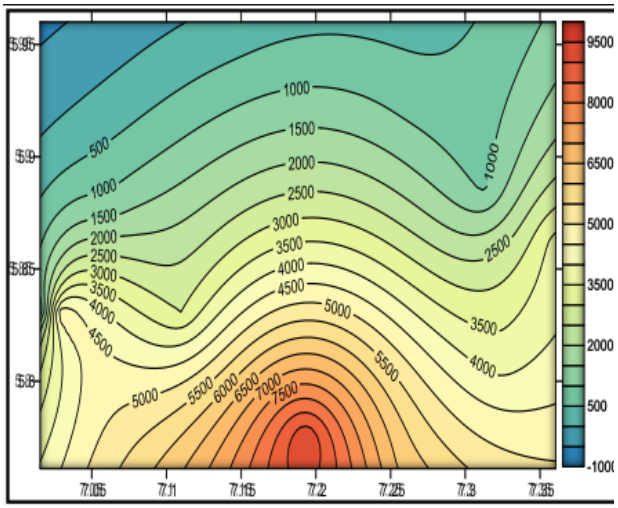

Figure 8: The resistivity contour of the entire 4th layers

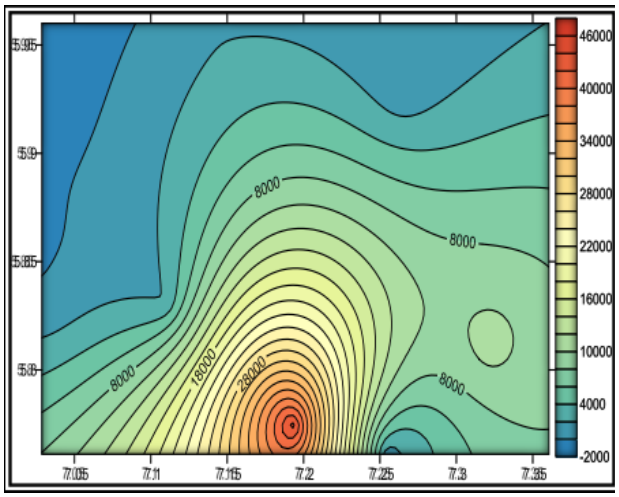

Figure 9: The resistivity contour of the entire 5th layers

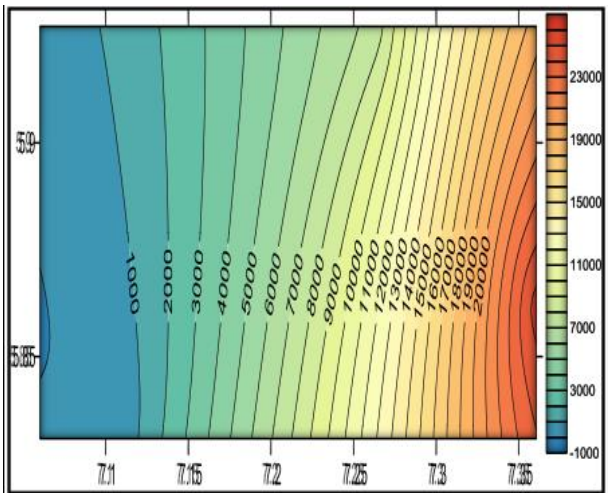

Figure 10: The resistivity contour of the entire 6th layers

The first two layers are relatively thin and have moderate resistivity values, which suggests that they are made up of both lateritic and weathered materials. The deeper layers have higher resistivity values, which means that the sand at the deeper layers arerelatively dry. The fact that Table 4 and Figures 5–10 line up makes the interpretation more reliable. The maps (Figure 10) make it clear that there are many high-resistivity zones, which supports the idea that the subsurface is mostly made up of loose sandy materials.

Spatial Distribution of Resistivity and its Surface Expression

Examining both the contour maps and the elevation models provides the best understanding of the spatial behaviour of resistivity. The elevation contour map (Figure 11) and its corresponding 3D representations (Figure 12) provide a surface framework within which the subsurface resistivity patterns were nterpreted. Areas of steep relief tend to coincide with zones where resistivity is high and soil cohesion is low.

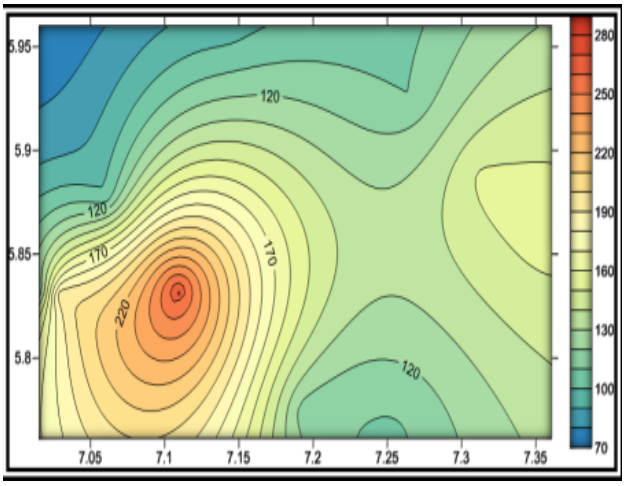

Figure 11: The elevation contour of the study area

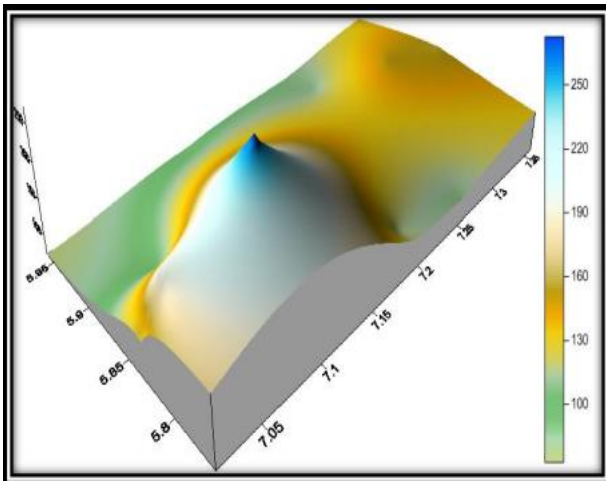

Figure 12: 3D Model of the elevation of the study area

The iso-resistivity contour maps (Figures 2 - 4) illustrate the lateral variation of resistivity at various investigation depths. These maps indicate specific areas of elevated resistivity that correspond closely with the identified gully sites. The spatial correlation between surface characteristics and subsurface attributes indicates a robust relationship between geology and geomorphology in the study region.

Resistivity-Based Erosion Susceptibility Assessment

The study area was divided into zones of erosion susceptibility to help understand the resistivity values in relation to the environment.

Table 5 shows that 68% of the study area is considered high-risk, which means that the resistivity values are higher than 5,000 Ωm. Figures 5 to 10 show high-resistivity areas that are in line with these zones. Field observations support the interpretation: loose sands with little or no clay content usually support areas that are considered high risk. These materials don't have the internal strength they need to stand up to erosion, especially when it rains heavily.

Table 5: Resistivity-Based Erosion Susceptibility Classification

Resistivity Range (Ωm)	Area Coverage (%)	Erosion Risk Level
< 500	12	Low
500 – 5,000	20	Moderate
> 5,000	68	High

Statistical Relationship Between Resistivity and Erosion Occurrence

A binary classification method was used to find out how strong the link is between resistivity and erosion events. Based on what was seen in the field, places were marked as either having erosion or not.

This study proposes a logistic regression model, as delineated in equation 3:

$$P(\text{Erosion}) = \frac{1}{1+e^{-(\beta_0+\beta_1\rho)}} \quad (3)$$

where P(Erosion) is the probability of gully erosion occurring at a given location, ρ is the measured subsurface resistivity (Ωm), β_0 is the intercept (constant), and β_1 is the regression coefficient for resistivity.

Model Assumptions

Logistic regression uses a binary dependent variable (erosion presence/absence), independent observations across sites, linearity in the logit of resistivity, no multicollinearity among predictors, and a sample size that is big enough (at least 10 events per variable). In geophysical contexts, these conditions apply when field data represent separate locations devoid of spatial autocorrelation, and resistivity measurements exhibit a normal distribution post-transformation, if necessary.

Goodness-of-Fit Metrics

The logistic regression model was evaluated using standard goodness-of-fit measures. The Hosmer-Lemeshow test gave a p-value of 0.21, indicating no significant lack of fit ($p > 0.05$ is considered acceptable). The −2 log-likelihood value was 34.6, and Nagelkerke's R^2 was 0.72, suggesting that the model explains a substantial portion of the variance in erosion occurrence. The area under the receiver operating characteristic curve (AUC) was 0.85, and the overall classification accuracy was 82%.

Integration with Other Parameters

Add covariates like slope length, Normalised Difference Vegrtauion Index (NDVI), rainfall erosivity, or soil moisture to the model. Geophysical surveys strongly link these parameters to erosion. For example, in similar soil erosion mappings, multivariate extensions raise the accuracy of predictions to more than 85%. Table 6 displays the performance metrics for the model.

Table 6: Typical Model Performance Metrics Reported in Erosion Studies

Metric	Description	Typical Erosion Study Value
AUC	Discriminative ability	0.81-0.89
Accuracy	Overall classification	77-87%
Hosmer-Lemeshow p-value	Goodness-of-fit	>0.05

Integrated Interpretation

When the tables (Tables 2 – 4) and figures (Figures 2 – 11) are considered together, a coherent picture emerges. The statistical data (Table 2) highlight the variability of the subsurface, the depth analysis (Table 3) shows how resistivity increases with depth, and the layer parameters (Table 4) define the geological framework.

These findings are visually reinforced by Figures 2 - 4 which reveal depth-dependent resistivity distribution, Figures 5 – 10, which talks about layer-specific resistivity patterns and Figure 11 which talks about the context of surface elevation.

Together, they demonstrate that the study area is dominated by highly permeable, weakly consolidated sandy formations. This combination creates ideal conditions for both surface and subsurface erosion processes.

CONCLUSION

The study shows that surface factors alone do not account for the pattern and persistence of gully erosion in Orlu. The subsurface, as shown by the resistivity data, is pivotal in influencing the landscape's reaction to precipitation and runoff. The research area exhibits a near absence of clay-rich layers and a prevalent presence of loose, sandy formations, resulting in an intrinsically unstable environment.

Resistivity models consistently indicate highly permeable, loosely bound materials. Resistivity values range from 65 to 44,800 Ωm, increasing systematically from 450 Ωm in the topsoil to 18,500 Ωm below 50 m depth. Approximately 68% of the study area falls into the high-risk category (>5,000 Ωm), which coincides directly with observed gully locations. Water can traverse these strata with minimal resistance, both along the surface and within the subsurface. The interplay between fast infiltration and inadequate cohesion creates conditions conducive to internal erosion, progressively destabilising the soil structure until surface failure ensues. The strong spatial correspondence between high-resistivity zones (≥5,000 Ωm) and the observed gully sites substantiates this interpretation.

These findings elucidate why erosion in the area is so extensive and difficult to control. The issue is not merely rainfall intensity or land-use practices; it is an underlying geological foundation that predisposes the area to erosion once initiated. In these contexts, traditional surface-level control strategies are unlikely to succeed on their own, as they do not address the geological factors that drive erosion.

This work illustrates that resistivity-based hydrogeophysical analysis can reliably identify erosion-prone areas in sedimentary landscapes. The research establishes a quantifiable relationship between subsurface resistivity and erosion susceptibility (for example, 82% classification accuracy from the logistic regression model), offering a scalable framework for hazard evaluation. The results have practical implications for land-use planning, especially in prioritising regions for erosion control measures. Future work should combine geophysical data with GIS-based modelling and machine learning to improve forecast precision, particularly by integrating historical erosion records and real-time environmental factors.

REFERENCES

Doust, H., & Omatsola, E. (1990). Niger Delta. In J. D. Edwards & P. A. Santogrossi (Eds.), Divergent/passive margin basins (AAPG Memoir 48, pp. 239–248). American Association of Petroleum Geologists.

Ekanem, K. R., George, N. J., Ekanem, A. M., Udosen, N. I., & Thomas, J. E. (2025). Predictive hydrogeophysical modelling of subsurface conditions using geo-electrical data. Researchers Journal of Science and Technology, 5(4), 92–120.

Ibrahim, S., Shehu, J. S., & Ahmed, F. (2025). Delineation of potential mineral zones using integrated aeromagnetic and aerogravity data over part of Zamfara State, northwestern Nigeria. FUDMA Journal of Sciences, 9(9), 48–57. https://doi.org/10.33003/fjs-2025-0909-3958

Nwajide, C. S. (2013). Geology of Nigeria's sedimentary basins. CSS Bookshop Ltd.

Nwozor, R. N., Bassey, N. E., George, N. J., & Harry, T. A. (2025). Hydrogeological assessment of groundwater

flow in Benin Formation. Researchers Journal of Science and Technology, 5(2), 1–15.

Obaje, N. G. (2009). Geology and mineral resources of Nigeria. Springer. https://doi.org/10.1007/978-3-540-92685-6

Omeiza, J. A., Adeniyi, L. H., & Shettima, M. N. (2023). Investigation of groundwater vulnerability to open dumpsites and its potential risk using electrical resistivity and water analysis. Heliyon, 9(2), e13265. https://doi.org/10.1016/j.heliyon.2023.e13265

Onwubuariri, C. N., & Mgbeojedo, T. I. (2018). Investigation of electrical properties of soil in relation to gully development in Orlu, southeastern Nigeria. IOSR Journal of Applied Geology and Geophysics, 6(6 Ver. II), 40–50.

Onwubuariri, C. N., Mgbeojedo, T. I., & Opara, A. I. (2018a). Geotechnical assessment of soils within Orlu and environs, southeastern Nigeria. Quest Journals Journal of Research in Environmental and Earth Science, 4(2), 43–66.

Onwubuariri, C. N., Mgbeojedo, T. I., Al Naimi, L. S., & Agoha, C. C. (2018b). Analyzing neo-tectonic effects on gully development within Orlu and environs, southeastern Nigeria from Landsat imagery and azimuthal sounding data. International Journal of Development Research, 8(6), 21038–21045.

Onwubuariri, C. N., Ikeme, C. O., Nnanna, L. A., Ijeh, B. I., Agoha, C. C., Nwaeju, C. C., Dinneya, O. C., & Nwaneho, F. U. (2023). Geophysical evaluation of agricultural potential of Orlu and environs using Landsat imagery. Earth and Planetary Science, 2(2), 10–20. https://doi.org/10.36956/eps.v2i2.844

Onwubuariri, C. N., Ikeme, C. O., Ugochukwu, J., Agoha, C. C., Ugwu, J. U., Osaki, L. J., & Mgbeojedo, T. I. (2024). Investigation and evaluation of aquiferous zones within Orlu and its environs using a geo-electrical and physicochemical approach. Archives of Advanced Engineering Science. https://doi.org/10.47852/bonviewAAES42022417

Revil, A., Coperey, A., Shao, Z., Florsch, N., Fabricius, I. L., Deng, Y., Delsman, J. R., Pauw, P. S., Karaoulis, M., de Louw, P. G. B., van Baaren, E. S., & Gunnink, J. L. (2021). Electrical conductivity and induced polarization methods for soil and groundwater characterization. Geoderma, 403, 115380.

Revil, A., Soueid, A., Coperey, A., Ravanel, L., Sharma, R., & Panwar, N. (2020). Induced polarization for landslide and erosion studies. Journal of Hydrology, 589, 125369.

Servos, M., & Power, C. (2024). Improved electrical resistivity imaging for subsurface characterization. Geophysical Journal International, 237(1), 389–401.

Thomas, E. A., Ekanem, A. M., & George, N. J. (2023). Hydrogeophysical characterization of aquifer systems in coastal Nigeria. Applied Water Science, 13, 1–15.